4-Fluorophenylglycine as a Label for ^{19}F NMR Structure Analysis of Membrane-Associated Peptides

Sergii Afonin,[a] Ralf W. Glaser,[b] Marina Berditchevskaia,[c] Parvesh Wadhwani,[a] Karl-Heinz Gührs,[d] Ute Möllmann,[e] Andrea Perner,[e] and Anne S. Ulrich*[a, c]

The non-natural amino acid 4-fluorophenylglycine (4F-Phg) was incorporated into several representative membrane-associated peptides for dual purpose. The ^{19}F-substituted ring is directly attached to the peptide backbone, so it not only provides a well-defined label for highly sensitive ^{19}F NMR studies but, in addition, the D and L enantiomers of the stiff side chain may serve as reporter groups on the transient peptide conformation during the biological function. Besides peptide synthesis, which is accompanied by racemisation of 4F-Phg, we also describe separation of the epimers by HPLC and removal of trifluoroacetic acid. As a first example, 18 different analogues of the fusogenic peptide "B18" were prepared and tested for induction of vesicle fusion; the results confirmed that hydrophobic sites tolerated 4F-Phg labelling. Similar fusion activities within each pair of epimers suggest that the peptide is less structured in the fusogenic transition state than in the helical ground state. In a second example, five doubly labelled analogues of the antimicrobial peptide gramicidin S were compared by using bacterial growth inhibition assays. This cyclic β-sheet peptide could accommodate both L and D substituents on its hydrophobic face. As a third example, we tested six analogues of the antimicrobial peptide PGLa. The presence of D-4F-Phg reduced the biological activity of the peptide by interfering with its amphiphilic α-helical fold. Finally, to illustrate the numerous uses of L-4F-Phg in ^{19}F NMR spectroscopy, we characterised the interaction of labelled PGLa with uncharged and negatively charged membranes. Observing the signal of the free peptide in an aqueous suspension of unilamellar vesicles, we found a linear saturation behaviour that was dominated by electrostatic attraction of the cationic PGLa. Once the peptide is bound to the membrane, however, solid-state ^{19}F NMR spectroscopy of macroscopically oriented samples revealed that the charge density has virtually no further influence on the structure, alignment or mobility of the peptide.

Introduction

Protein–lipid interactions are of fundamental relevance to cellular processes occurring at the plasma membrane and organelles. For example, antimicrobial peptides are used by many organisms as a first-line defence, as they are able to permeabilise the membranes of invading bacteria.[1] Fusogenic peptides represent the minimal membrane-perturbing part of various proteins that are involved in inter- and intracellular fusion processes.[2] Many different amphiphilic peptides and proteins interact permanently or reversibly with membranes, to operate as ion channels, transporters, toxins, enzymes, etc. As a functional picture of these systems is beginning to emerge, new experimental strategies are needed to study the structure and dynamics of peptides when they are bound to the lipid bilayer.

Fluorescence and electron paramagnetic resonance spectroscopy are sensitive methods commonly used to characterise peptides in membranes. In many cases, however, bulky labels have to be incorporated, which may affect the peptide–lipid interactions studied. Depending on the mode of attachment, a flexible reporter group may not reflect the behaviour of the labelled molecule that well. Nonperturbing methods, such as solid-state NMR spectroscopy with selective ^{2}H, ^{13}C or ^{15}N labels, on the other hand, are highly informative but are not very sensitive as they require comparatively large amounts of material.[3] Protons are, of course, the most sensitive reporters, but in view of their natural abundance it is not yet feasible to investigate membrane-bound peptides by solid-state ^{1}H NMR

[a] Prof. Dr. A. S. Ulrich, S. Afonin, Dr. P. Wadhwani
Forschungszentrum Karlsruhe, IFIA
P.O.B. 3640, 76021 Karlsruhe (Germany)
Fax.: (+49) 721-608-4823
E-mail: anne.ulrich@ifia.fzk.de

[b] Dr. R. W. Glaser
Institute für Biochemie und Biophysik
Friedrich-Schiller-Universität Jena
Hans-Knöll-Strasse 2, 07745 Jena (Germany)

[c] Prof. Dr. A. S. Ulrich, Dr. M. Berditchevskaia
Institut für Organische Chemie, Universität Karlsruhe
Fritz-Haber-Weg 6, 76131 Karlsruhe (Germany)

[d] Dr. K.-H. Gührs
Institut für Molekulare Biotechnologie
Beutenbergstrasse 11, 07745 Jena (Germany)

[e] Dr. U. Möllmann, A. Perner
Hans-Knöll-Institut für Naturstoff-Forschung e.V.
Beutenbergstrasse 11a, 07745 Jena (Germany)

 DOI: 10.1002/cbic.200300568 © 2003 Wiley-VCH Verlag GmbH & Co. KGaA, Weinheim

spectroscopy. Hence, a good compromise for studying peptide–lipid interactions is offered by ^{19}F NMR spectroscopy, for which suitable fluorine labels need to be selectively incorporated. The sensitivity of the ^{19}F nucleus is nearly as high as that of the proton, and there is no natural background. The strong dipolar couplings of the ^{19}F nucleus provide intra- or intermolecular distances in solids of up to 12 Å, and the large chemical shift anisotropy is very useful for analysing molecular orientations.[4] When a single proton is replaced by a ^{19}F atom, the structural implications are expected to be small.[5] Fluorine NMR labels have been successfully used to study peptides and proteins both in solution and in the membrane-bound state.[6] ^{19}F NMR spectroscopy has also been applied to characterise the binding of fluorine-containing drugs and anaesthetics to lipid membranes.[4a, 7]

The non-natural amino acid 4-fluorophenylglycine (4F-Phg) is explored here as a label for ^{19}F NMR studies of membrane-associated peptides. The advantage of 4F-Phg over any of the commonly used fluorinated amino acids lies in the stiff connection of the *para*-fluoro substituent to the peptide backbone. In all natural amino acids with a proton replaced by a fluorine atom (such as Phe, Trp, Tyr or Leu) the position of the label with respect to the peptide backbone would depend on the side-chain conformation, which is not usually known in membrane peptides. The special side-chain architecture of 4F-Phg recently enabled us to deduce the backbone conformation of membrane-bound gramicidin S from the intramolecular ^{19}F–^{19}F dipolar coupling between two 4F-Phg reporter groups.[6b] The same study also enabled us to determine the alignment and mobility of the entire peptide in the lipid bilayer. Even though 4F-Phg is not a common building block in biology, phenylglycine and its derivatives have found numerous applications as components of semisynthetic antibiotics, artificial sweeteners, enzyme inhibitors and immobile phases for chiral chromatography, amongst others.[8] Phenylglycine is even part of some natural antibiotics, like pristinamycin I and virginiamycin S.[9] The aromatic β branch in phenylglycine may favour a different preferential conformation in the protein backbone compared to any standard amino acid. Computer modelling studies have shown that its global energy minimum corresponds to a nearly extended β-strand conformation, while a right-handed α helix is less stable by about 1.3 kcal mol^{-1}.[10] Nevertheless, the available conformational space is almost as large as for alanine, and hence, L-4F-Phg promises to be a relatively nonperturbing side chain. When the D enantiomer is incorporated into a protein, on the other hand, we expect that any intrinsic steric effects will be enhanced due to the stiffness of the bulky side chain.[11]

Here, we assess the conformational and functional consequences of incorporating an L- or D-4F-Phg side chain into a representative range of systems. Three types of membrane-active peptides with distinctly different structures were selected whose biological functions have been well described in the past. The first antimicrobial sequence, PGLa, shares characteristic features with other cationic peptides from the magainin family.[12] They are unfolded in aqueous solution but convert into an amphiphilic α helix upon membrane binding (Figure 1, bottom).[1, 13] The second type of antimicrobial peptide investigated here, gramicidin S, is also cationic and exhibits an overall amphiphilic character, but this cyclic decapeptide forms an antiparallel β sheet (Figure 1, top).[6b, 14] By comparing the behaviour of the sterically constrained 4F-Phg side chain in these two representative types of secondary structure, its compatibility with the peptide backbone is systematically evaluated. In addition, we have included in this study a third kind of peptide, B18, which is derived from a sea urchin sperm protein and mediates fertilisation by triggering membrane fusion.[15] Like most other fusogenic sequences, this peptide exhibits a pronounced conformational plasticity in lipid membranes.[2, 16] It is able to assume either an α-helical or an oligomeric β-sheet structure, depending on the lipid environment and sample history.[17] Only recently we resolved its helix–turn–helix structure in the membrane-bound state by solid-state ^{19}F NMR analysis of the 4F-Phg-labelled analogues described here.[6d]

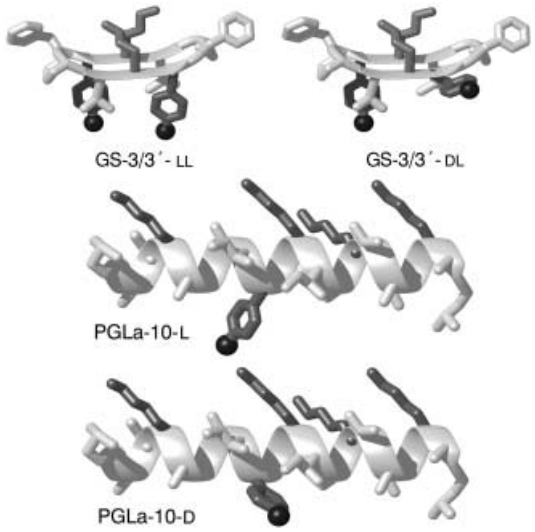

Figure 1. Model structures of the cyclic β-sheet gramicidin S analogues GS-3/3′-LL and GS-3/3′-LD, and of the α-helical PGLa analogues PGLa-10-L and PGLa-10-D. Charged ornithine and lysine side chains as well as 4-fluorophenylglycine side chains are shown in dark grey, and the fluorine atom is shown in black. The PGLa structures were derived from an idealised α-helical conformation by simple energy minimisation. The figure was produced with the MOLMOL[36] and POVRAY programs.

Altogether, we have introduced 4F-Phg into more than 30 analogues of the three peptides B18, gramicidin S and PGLa, in order to study their respective conformations, membrane interactions and biological activities. The analogues are listed in Table 1, which specifies our nomenclature and the stereochemistry of D- or L-4F-Phg at the substituted positions. The results presented here summarise the general aspects of peptide synthesis and purification, especially with regard to racemisation of 4F-Phg. Structural studies as well as functional tests of the antimicrobial or fusogenic activities are used to demonstrate that 4F-Phg labels are well suited for structure analysis by ^{19}F NMR spectroscopy. Finally, we have examined the role of electrostatics on the lipid–protein interactions of the antimicrobial peptide PGLa, in order to illustrate the various NMR spectroscopy techniques that can be usefully applied to such ^{19}F-labelled peptides.

 © 2003 Wiley-VCH Verlag GmbH & Co. KGaA, Weinheim

Table 1. Wild-type peptides and their 4F-Phg-labelled analogues prepared for this study.

Analogue name	Label	4F-Phg conformation
B18: fusogenic peptide, highly conserved sequence of the sea urchin fertilisation protein Bindin, numbered as in *Strongylocentrotus purpuratus*. NH_2-Leu[103]GlyLeu[105]Leu[106]Leu[107]ArgHisLeu[110]ArgHisHisSerAsnLeu[116]Leu[117]-Ala[118]AsnIle[120]-COOH		
B18-103	Leu103 to 4F-Phg	L[a]
B18-105	Leu105 to 4F-Phg	L, D
B18-106	Leu106 to 4F-Phg	L, D
B18-107	Leu107 to 4F-Phg	L, D
B18-110	Leu110 to 4F-Phg	L, D
B18-116	Leu116 to 4F-Phg	L, D
B18-117	Leu117 to 4F-Phg	L, D
B18-118	Ala118 to 4F-Phg	L, D
B18-106/116	Leu106 and Leu116 to 4F-Phg	LL, LD/DL, DD
PGLa: antimicrobial peptide from frog skin, identified in *Xenopus laevis* NH_2-GlyMetAlaSerLysAlaGlyAla[8]IleAla[10]GlyLysIle[13]AlaLysValAlaLeuLysAla-Leu-$CONH_2$		
PGLa-8	Ala8 to 4F-Phg	L, D
PGLa-10	Ala10 to 4F-Phg	L, D
PGLa-13	Ile13 to 4F-Phg	L, D
gramicidin S: antimicrobial cyclic peptide from *Bacillus brevis* [Val[1]OrnLeu[3]D-PheProVal[1′]OrnLeu[3′]D-PhePro]$_{cyclo}$		
GS-1/1′	Val1 and Val1′ to 4F-Phg	LL, LD, DD
GS-3/3′	Leu3 and Leu3′ to 4F-Phg	LL, LD

[a] Single peak observed by HPLC, as the N-terminal 4F-Phg may not have undergone racemisation.

Results and Discussion

Racemisation of 4-fluorophenylglycine

It is well known that the aromatic side chain of phenylglycine makes the α-carbon atom of this amino acid sufficiently acidic to be readily deprotonated by any weak base used during 9-fluorenylmethoxycarbonyl (Fmoc) solid-phase peptide synthesis. Besides favourable electron delocalisation, in 4F-Phg the α-carbanion species is further stabilised by the presence of the electronegative *para*-fluoro substituent. Racemisation via a trigonal α-carbon intermediate is thus virtually inevitable when L-4F-Phg is introduced into peptides by standard Fmoc chemistry. We tested several modifications of the protocol, as the extent of racemisation is known to be influenced by the tertiary base employed for coupling.[18] When 2,4,6-collidine was used in combination with 2-(1*H*-benzotriazole-1-yl)-1,1,3,3-tetramethyluronium hexafluorophosphate (HBTU) to couple both 4F-Phg and the subsequent amino acid, we managed to suppress racemisation to about 15% by lowering the temperature to 0 °C with a reaction time of 15 minutes. However, the coupling efficiency was significantly reduced to about 60–70%, and hence, the overall yield of the all-L peptide was not increased. We also tested tetramethylfluoroformamidinium hexafluorophosphate (TFFH),[18, 19] bis-(tetramethylenefluoroformamidinium) hexafluorophosphate (BTTFH)[19] and cyanuric fluoride[20] for their ability to incorporate 4F-Phg into test peptides without racemisation. Out of the many peptide-coupling reagents described in the literature, we selected these three acid fluorides because of their long shelf-life and rapid acting ability. In a related project, TFFH in the presence of collidine provided optimal conditions for incorporating 3-fluoroalanine (which easily eliminates HF) into a test peptide. With 4F-Phg, however, we were unable to achieve a satisfactory suppression of racemisation.

Since racemisation could not be avoided, chromatographic resolution of the two epimeric products containing L- and D-4F-Phg was crucial. Fortunately, for all of our peptides synthesised so far the retention times during reversed-phase HPLC were sufficiently different to allow separation and purification of the peptides in milligram amounts. Therefore, we used the inexpensive racemic mixture of D/L-4F-Phg for peptide synthesis and did not pay any further attention to racemisation. In fact, the "unwanted" epimer that is obtained as a byproduct (that is, the peptide containing D-4F-Phg) proved to be highly useful for comparative structural and functional studies, as discussed below. There was no general rule with respect to the order in which the epimers eluted from the reversed-phase HPLC column.[11a, 21] In all PGLa samples and in B18-110 the D-4F-Phg epimer eluted first, while in all other B18 samples the L-4F-Phg epimer eluted first. In all gramicidin S analogues the order was DD, DL, LL, according to increasing amphiphilicity.

The configuration of the 4F-Phg in each pair of epimers was assigned by using Marfey's reagent after acid hydrolysis of the peptide.[22] The reversed-phase HPLC profiles of the derivatised amino acids exhibit distinct peaks for the two enantiomers of 4F-Phg, as illustrated in Figure 2. During hydrolysis a partial racemisation occurred again. For the two epimer fractions of any singly substituted peptide we nevertheless obtained an unambiguous and reproducible assignment, with a significant excess of the L-4F-Phg derivative in one fraction or of the D-4F-Phg derivative in the other. Only the doubly labelled gramicidin S peptide yielded three major HPLC peaks of the correct molecular weight that could not be unambiguously assigned by derivatisation with Marfey's reagent alone. In this case, high-resolution ^{19}F NMR spectroscopy in methanol was used to identify the

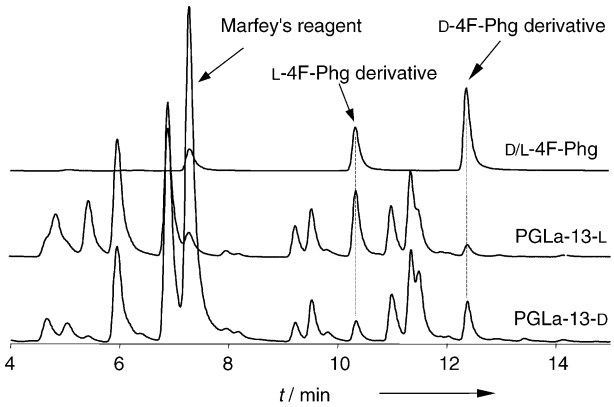

Figure 2. HPLC chromatograms monitored at 415 nm of D/L-4F-Phg and of the two epimers of PGLa-13 after acid hydrolysis and derivatisation with Marfey's reagent. The two purified PGLa analogues containing L- and D-4F-Phg can be unambiguously assigned, despite partial racemisation during the derivatisation procedure.

 © 2003 Wiley-VCH Verlag GmbH & Co. KGaA, Weinheim

asymmetric DL stereoisomer by its two distinct NMR signals, in contrast to the symmetric LL and DD stereoisomers, which gave a single NMR signal each.

Once the epimerically pure peptides had been obtained, no further racemisation could be detected under standard conditions of sample preparation, storage and NMR measurements. We reextracted four PGLa analogues and one gramicidin S analogue from reconstituted membrane samples, which had been incubated for 2–8 days at 48 °C and had been exposed during NMR experiments to temperatures of 15–55 °C for up to 4 days. None of the peptides contained any significant amount of the unwanted epimer. Even after storage for a year at 8 °C we detected no chemical degradation for GS-3/3′ in 1,2-dimyristoyl-*sn*-glycero-3-phosphocholine (DMPC). (No bacterial decay was detected either as the peptide itself is an antibiotic.)

Removal of trifluoroacetic acid from the peptides

Trifluoroacetic acid (TFA) is commonly used to cleave peptides from the resin and to enhance resolution in reversed-phase HPLC. In synthetic peptides from various sources we always detected significant amounts of TFA, in up to 5-fold molar excess. TFA gives rise to a strong signal in ^{19}F NMR spectra at around $\delta = -75$ ppm, which overlaps with the downfield edge of the static chemical-shift anisotropy (CSA) tensor of the 4F-Phg label (about $\delta_{11} = -62$ ppm, $\delta_{22} = -125$ ppm, $\delta_{33} = -154$ ppm).[6b,d] This becomes less of a problem when the CSA is narrowed down by fast motional averaging of the whole peptide in the bilayer or of the 4F-Phg side chain around its $C\alpha$–$C\beta$ bond. Nonetheless, we were further concerned with removing TFA from the samples, because we noticed several signs of tight binding between TFA and the peptides. One of these signs was the difficulty in removing TFA, as described below, and another indication was the difference in the ^{19}F NMR signal of TFA in the absence and presence of peptide. Briefly, the TFA signal in macroscopically oriented membranes in the fluid phase is a triplet, resulting from the ^{19}F dipolar interactions within the aligned CF_3 group.[4a] We prepared TFA-containing samples in DMPC/1,2-dimyristoyl-*sn*-glycero-3-[phospho-*rac*-(1-glycerol)] (DMPG) without any peptide. Their spectra showed contributions from several triplets with variable intensities, depending on the temperature, charge and hydration of the membrane. Under typical conditions, with the sample normal aligned, parallel to the static magnetic field, the chemical shift was between −69 and −73 ppm, and the dipolar coupling was 800–2000 Hz. TFA also gave rise to a triplet in the same range in the presence of peptide, but with significantly different coupling values and chemical shifts that depended on the type of peptide. Interestingly, when added to DMPC in the gel phase, TFA gave a single isotropic signal at $\delta = -75$ ppm; hence, we conclude that TFA gets expelled from the membrane when the acyl chains rigidify.

Since the strong ion-pairing effect of TFA may modify the interaction of amphiphilic peptides with the membrane, we took care to replace TFA by less strongly bound anions such as Cl^-, even for the ^{1}H NMR and circular dichroism experiments where TFA is not usually considered to be a problem. The same precautions are essential for FT-IR measurements, as the COO^- stretching vibration of TFA overlaps with the amide I band of the peptides.[23] Several methods are commonly used to remove residual TFA: 1) purification over ion-exchange resins, 2) vacuum drying over P_2O_5 or 3) lyophilisation from solutions of other volatile acids. We found that TFA could be removed on an amberlite ion-exchange column, but the method suffered from incomplete recovery of peptide. Vacuum drying over P_2O_5 removed excess free TFA but not the TFA^- counterions bound to the cationic peptides. Repeated lyophilisation from dilute HCl or acetic acid solutions reduced the content of TFA, but it was still detectable after 3 cycles (each with a 100-fold molar excess of acetic acid over peptide). Therefore, we optimised the reversed-phase HPLC peptide purification protocol by using solvents with different ion-pairing agents, like hydrochloric, formic or phosphoric acid. We recommend this as the most efficient technique to remove TFA. With 5 mM HCl in the aqueous phase of the HPLC gradient, a peak separation is achieved comparable to 0.1 % TFA. Note that HCl must not be added to the organic phase because mixtures of HCl with acetonitrile or methanol are very corrosive. Special precautions should also be taken when lyophilising the HPLC fractions to prevent condensation of HCl in the pump. (See Experimental Section for details.)

UV absorption of the aromatic 4F-Phg side chain

Purified peptides are difficult to handle after lyophilisation because of electrostatic problems, and in addition they may contain unknown amounts of water and salt. Therefore, peptide concentrations were determined from the UV absorption of their aromatic side chains. When incorporated into a protein, 4F-Phg shows a maximum absorption at around 263 nm, as illustrated in Figure 3. The free amino acid cannot be used for calibration

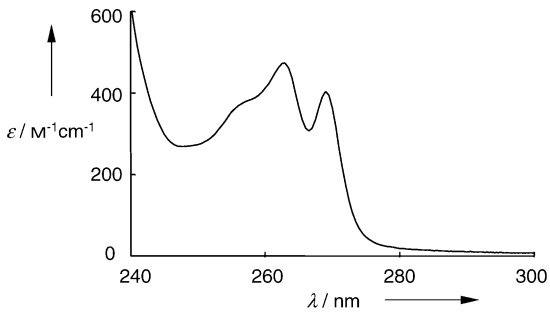

Figure 3. UV spectrum of PGLa-10-L in aqueous buffer. The aromatic region of the 4F-Phg side chain is shown. The spectrum is scaled to display directly the molar absorption coefficient ε.

because its molar absorption coefficient depends strongly on the protonation state. Absorption of free 4F-Phg increases from 350 M^{-1} cm^{-1} at acidic pH to 660 M^{-1} cm^{-1} at alkaline pH, and the peak shifts by about 4 nm to a higher wavelength. To calibrate the molar absorption coefficient of 4F-Phg within a peptide, we first determined the peptide concentration in D_2O by integrating selected ^{1}H NMR signals, which were in turn calibrated against solutions of organic molecules of known concentration. The

 © 2003 Wiley-VCH Verlag GmbH & Co. KGaA, Weinheim

molar absorption coefficient of 4F-Phg in the peptides at 263 nm was thus determined to be $473 \pm 13\,\mathrm{M}^{-1}\,\mathrm{cm}^{-1}$. There were no significant differences between the absorption coefficients in different types of peptides or between the analogues containing 4F-Phg in different positions.

The effect of 4-fluorophenylglycine on helical structure

To evaluate the suitability of the 4F-Phg side chain as a label to study the orientation and dynamics of peptides in a membrane environment we checked whether the replacement of a hydrophobic amino acid with 4F-Phg changed the structure or the function of the peptides. The secondary structure of the PGLa analogues was studied by circular dichroism (CD) spectroscopy in the presence of lipid vesicles or 30% trifluoroethanol (TFE) and was compared with wild-type PGLa (data not shown). The CD line shapes of all these peptides were very similar and showed a high content of α-helical structure. The D-4F-Phg analogues exhibited, on average, a signal that was about 10% less negative at 222 nm than the signals of those analogues labelled with L-4F-Phg, a result which indicates a slightly lower degree of α helix.

The CD measurements are not sensitive enough to detect local changes in the structure that affect only one or two residues. Therefore we studied three of the peptides (wild-type PGLa, PGLa-10-L and PGLa-10-D) with two-dimensional ^{1}H–^{1}H high-resolution NMR spectroscopy in 30% TFE. We did not attempt to determine the complete structure of the PGLa peptides from distance constraints because there are no long-range NOE cross-peaks and the peptides appear to be quite flexible. As we had shown in the case of B18,[17a] under such conditions the structure calculation strongly depends on individual distance constraints that can or cannot be resolved from overlapping resonances in the NOESY spectra, and it is difficult to judge whether small variations in the resulting structures are significant. A comparison of the individual NOE intensities (not shown) and the chemical shifts (Figure 4) shows that all three peptides form an α helix that is well defined in the C-terminal region and less defined in the N-terminal part, as had

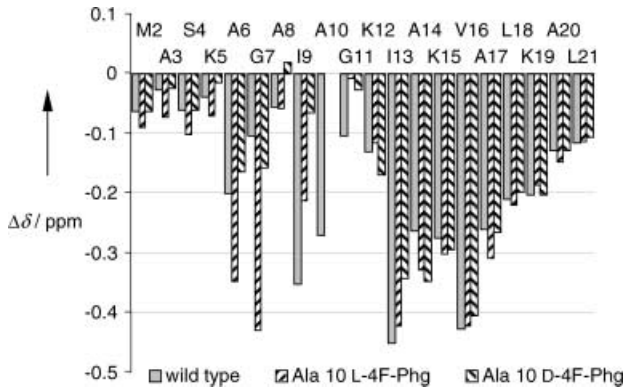

Figure 4. Chemical shift difference Δδ of the Hα protons of wild-type PGLa and its analogues with L- and D-4F-Phg in the position of Ala10, relative to the "random coil" chemical shift of the respective amino acid in a GGXGG peptide. Negative values (upfield shifts) indicate α-helical structure.[41]

been found for wild-type PGLa in dodecyl phosphocholine micelles.[12] Neither L- nor D-4F-Phg break the α-helical structure; this is indicated by changes in the NOE intensity being small for HA_i–HN_{i+3} and other cross-peaks that characterise helical structure in the environment of the 4F-Phg label.

The ^{1}H chemical shifts and NOE cross-peak intensities also provide information about side-chain dynamics. We observe only one sharp *J*-coupling pattern each for the H_γ and the H_δ protons of the aromatic 4F-Phg ring, which indicates a fast ring flip on the NMR timescale. In PGLa-10-L the NOE cross-peaks between the aromatic ring protons and the Ile13 side chain and towards the Gly7 and Gly11 H_α protons are stronger than in PGLa-10-D, where the NOE interactions to the Ile9 side chain are stronger. This pattern is in good qualitative agreement with the structural model shown in Figure 1. The chemical shifts of the side-chain protons in the environment of the 4F-Phg label are also in agreement with this model, although the differences with respect to the wild-type peptide are only about one third of the ring-current shifts expected for a static phenylalanine ring (Table 2). We think that the ring-current effects of Phe and 4F-Phg are quite similar and that the smaller shifts are mainly due to a high flexibility of the side chain. These data together indicate that the incorporation of L-4F-Phg does not significantly disturb an α-helical peptide sequence, while D-4F-Phg incorporation requires some structural adaptation and slightly destabilises the α helix, but does not act as a strong α-helix breaker.

Table 2. Selected chemical shifts of wild-type PGLa and its analogues with L- and D-4F-Phg in the position of Ala10.[a]

	Measured ^{1}H chemical shift of PGLa analogues [ppm]			Predicted 4F-Phg ring-current shift[b] [ppm]	
	wild-type	PGLa-10-L	PGLa-10-D	PGLa-10-L	PGLa-10-D
Ala6 Hα	4.14	3.99	4.18	−0.21	0.10
Gly7 Hα	3.91	3.42/3.74	3.80/3.90	−1.14/−0.23	0.04/0.06
Ala8 Hα	4.28	4.28	4.36	0.03	0.06
Ile9 Hα	3.83	3.97	4.11	0.04	−0.01
Gly11 Hα	3.90	4.00	3.95/4.02	0.14/0.15	0.13/0.08
Lys12 Hα	4.19	4.20	4.15	0.05	−0.03
Ile13 HN	8.26	8.12	7.85	0.12	−0.32
Ile13 Hα	3.73	3.76	3.84	0.04	−0.24
Ile13 Hβ	1.97	1.98	1.52	0.11	−1.64
Ile13 Hγ1	1.77/1.19	1.84/1.21	1.41/1.24	0.05/0.09	−0.41/−0.62
Ile13 Qδ1	0.85	0.92	0.76	0.10	−0.95
Ile13 Qγ2	0.93	0.92	0.77	0.02	−0.28
Ala14 Hα	4.08	4.01	3.99	−0.05	0.07
Ala14 Qβ	1.53	1.46	1.42	−0.07	0.10

[a] Measured in 30% TFE. The protons are not stereospecifically assigned. [b] The ring-current shifts calculated for the energy-minimised structures shown in Figure 1.

Fusion activities of the B18 peptide analogues containing 4F-Phg

In the fusogenic peptide B18 we substituted each hydrophobic

 © 2003 Wiley-VCH Verlag GmbH & Co. KGaA, Weinheim

position—one at a time—with 4F-Phg and thus targeted Leu seven times and Ala once. (One L- and one D-4F-Phg-containing analogue was usually produced in each case.) In an additional sequence, two Leu residues (106 and 116) were substituted with 4F-Phg simultaneously. The functional activity of the 18 purified peptide analogues (singly and doubly labelled stereoisomers, see Figure 5) was tested with a fluorescence dequenching assay,

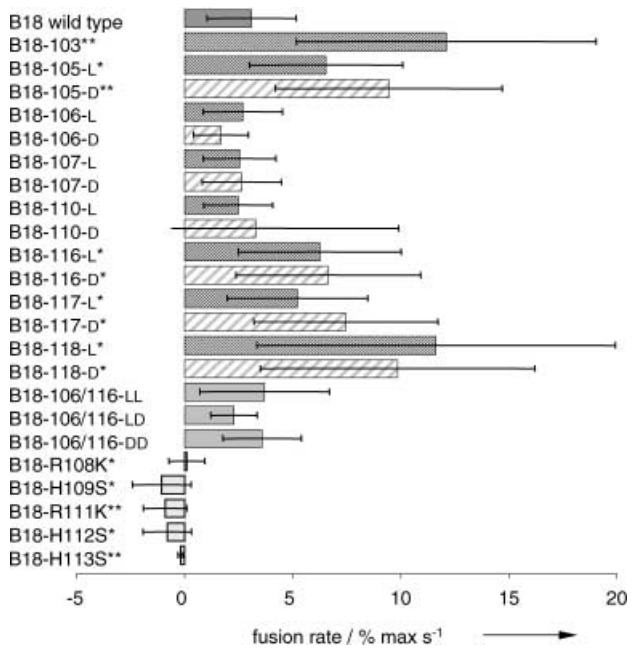

Figure 5. *Fusogenic activity of the B18 analogues compared with the wild-type peptide, monitored by a fluorescence dequenching assay. Statistically significant deviations from the activity of wild-type B18 are labelled * for $<5\%$ and ** for $<0.5\%$ significance level according to a two-tailed Student's t-test.*

which quantifies the peptide-induced fusion of large unilamellar lipid vesicles.[15b] For comparison, we also tested five additional B18 analogues in which a single hydrophilic amino acid had each been conservatively substituted ($3\times$ His $\rightarrow$ Ser and $2\times$ Arg $\rightarrow$ Lys). The results are summarised in Figure 5.

All peptide analogues in which hydrophobic amino acids were replaced by 4F-Phg retained the fusogenic activity of B18. Substitutions in the centre of the peptide did not affect the rate of fusion significantly, while 4F-Phg near the N or C terminus even increased the activity. In contrast, any of the seemingly conservative replacements of His $\rightarrow$ Ser or Arg $\rightarrow$ Lys virtually abolished fusion. ^{19}F-labelling at the hydrophobic sites is thus tolerated by the peptide, whereas the polar side chains appear to play more specific functional roles in B18.[15, 23] Having thus verified the functional integrity of the whole set of 4F-Phg-labelled peptides, we recently used solid-state ^{19}F NMR spectroscopy to determine the membrane-bound structure of the B18 sequence after fusion; this showed a "boomerang"-like immersion of the helix – turn – helix structure in the lipid bilayer.[6d]

Remarkably, in Figure 5 there are no significant or systematic differences in the fusion activities within any pair of epimeric peptides containing L- and D-4F-Phg. This observation allows a novel conclusion about the functional mechanism of peptide-induced fusion, namely that B18 must be rather unstructured and flexible at the moment of action. If the transition state had to assume either the well-defined α-helical or the self-aggregated β-sheet conformation described for B18 under equilibrium conditions, different fusion rates would have been expected for the D and L epimers due to their distinct steric preferences.[15b, 17]

Antimicrobial activities of the α-helical and β-sheet peptides

For comparative analysis we selected two representative antimicrobial peptides with characteristically different secondary structures, namely the α-helical peptide PGLa and the β-sheet peptide gramicidin S. PGLa was labelled with a single 4F-Phg substitution at three different positions in the central region of the molecule (Ala8, Ala10 and Ile13). Within the putative amphiphilic α helix, Ile13 and Ala10 are part of the hydrophobic surface while Ala8 lies within a partially polar region (Figure 1). The cyclic peptide gramicidin S was doubly labelled with 4F-Phg, such that the two substituents symmetrically replace either both Val or both Leu residues on the hydrophobic face of the amphiphilic molecule (Figure 1). To test the biological functions of the substituted PGLa and gramicidin S peptides, we examined the inhibition of bacterial growth by using two different protocols.

By means of an agar diffusion assay,[24] the antimicrobial activities of the peptides were monitored against different species and strains of Gram-positive and Gram-negative bacteria, as summarised in Figure 6. These semiquantitative results were substantiated quantitatively by determining the minimum inhibitory concentration (MIC) values[25] against *Escherichia coli* and *Staphylococcus aureus*; the results are listed in Table 3. Between the MIC values and the radius of inhibition in the agar diffusion tests, we found a correlation coefficient of 0.9, which confers a high confidence to the agar diffusion tests. When interpreting the inhibition experiments, it is important to take into account the ratio between the free peptide in the bacterial suspension and the peptide bound to or taken up by the bacteria. We systematically varied this ratio and determined the MIC values of wild-type gramicidin S and PGLa with an initial inoculum of *E. coli* of 5×10^3, 5×10^4 and 5×10^5 colony-forming units (CFU) mL^{-1} and of *S. aureus* of 5×10^4, 5×10^5 and 5×10^6 CFU mL^{-1}. The resulting MIC values differed by less than one step of dilution, which corresponds to a factor of two (data not shown). This proves that the amount of peptide consumed by the bacteria is small, and hence, the MIC data truly reflect the free concentration of peptide necessary to inhibit bacterial growth as discussed below.

For both PGLa and gramicidin S it is seen that the 4F-Phg-labelled analogues exhibit a pattern of activity against the widely differing strains of bacteria which is very similar to that exhibited by the respective wild-type peptides. This qualitative correspondence confirms that 4F-Phg substitution does not affect the fundamental mechanism of antimicrobial action. Quantitatively, however, some interesting variations are apparent. While the activities of the PGLa analogues containing L-4F-Phg do not differ much from the wild-type peptide, the D-4F-Phg epimers are

 © 2003 Wiley-VCH Verlag GmbH & Co. KGaA, Weinheim

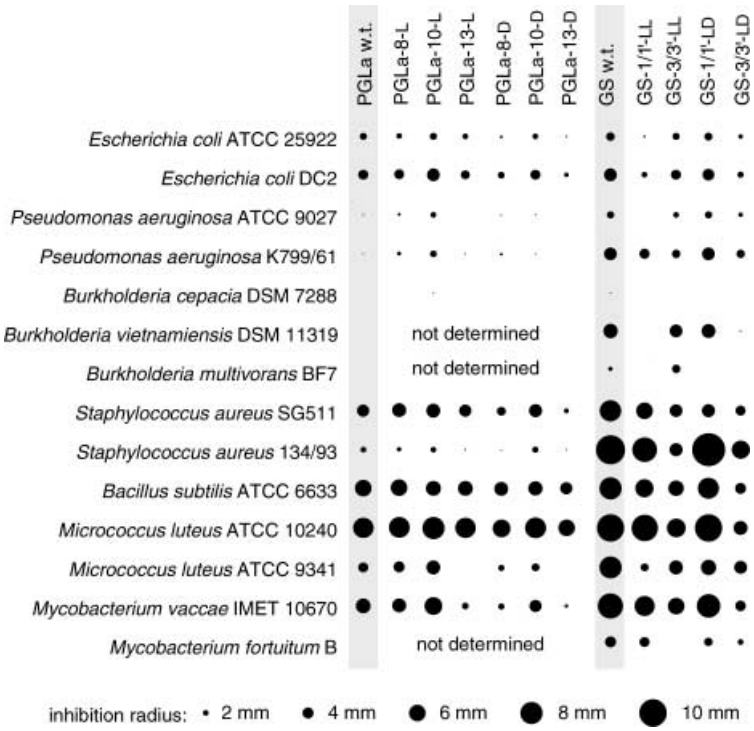

Figure 6. *Antimicrobial activity of PGLa and gramicidin S analogues against a variety of bacterial strains. The radius of the dot is proportional to the width of the inhibition zone surrounding the hole in the agar plate (inhibition radius = radius of inhibition zone − radius of hole) that was filled with a solution (100 μg mL^{-1}) of the test peptide. w.t. = wild-type peptide.*

Table 3. *Minimal inhibitory concentration (MIC) values of PGLa, gramicidin S, and their 4F-Phg-substituted analogues.*

Peptide	MIC [mg L^{-1}]	
	E. coli ATCC 25922	*S. aureus* SG 511
wild-type PGLa	6	1.5
PGLa-8-L	6	1.5
PGLa-8-D	12	6
PGLa-10-L	3	1.5
PGLa-10-D	6	3
PGLa-13-L	6	3
PGLa-13-D	25	12
wild-type GS	3	0.8
GS-1/1′-LL	12	3
GS-1/1′-LD	12	1.5
GS-1/1′-DD	> 25	> 12
GS-3/3′-LL	25	1.5
GS-3/3′-LD	12	1.5

consistently less active. This finding agrees well with the expectation that the rigid side chain of the D enantiomer would cause steric interference in a straight α helix,[11, 12, 21, 26] as discussed above.

The reduced antimicrobial activities of the D-4F-Phg-labelled PGLa analogues are thus attributed to their slightly lower tendency to form an α helix upon membrane binding. Previous studies of a similar antimicrobial peptide have reported a similar effect when two consecutive amino acids were substituted by their D enantiomers.[11b, 27] It appears reasonable that the steric consequences of the stiff β-branched D-4F-Phg should be more pronounced than for any D enantiomer of a natural amino acid (other than Pro). *All*-D analogues of magainin, a related antimicrobial peptide, showed the same antimicrobial activity as the natural *all*-L peptide.[28] It was concluded that the peptides act directly on the lipid membrane and do not require a receptor protein. This supports the interpretation that the influence of D-4F-Phg on the antibacterial action by D-4F-Phg results from the modified overall physico-chemical properties and not from the disturbance of a receptor interaction.

For most of the doubly labelled analogues of gramicidin S, the MIC values in Table 3 reflect somewhat decreased activities, by up to two titration steps compared to the wild-type peptide. From a structural point of view, the cyclic peptide should be able to accommodate both 4F-Phg enantiomers equally well in its antiparallel β-sheet backbone. Figure 1 illustrates that a D-amino acid in positions 1, 3, 1′ or 3′ (in our nomenclature) will point sideways away from of the hydrogen-bonded core. The CD spectra of our 4F-Phg analogues are indeed very similar to that of the wild-type peptide.[6b] In contrast, placing a D-amino acid at positions 2 or 2′ has been shown to disrupt the cyclic hydrogen-bonded structure of gramicidin S.[14b,c] In our series of peptides we had expected that the amphiphilic character would be more disturbed by D-4F-Phg than by L-4F-Phg and that this might show up in differential activities. However, Figure 6 and Table 3 do not reveal any systematic differences between the LL and DL epimers. Only the DD stereoisomer was found to be inactive. It thus appears that the peptide is just as sensitive towards the replacement of two hydrophobic side chains as it is to their stereochemistry. The reduced activity of the 4F-Phg-labelled peptides may be related to their solubility in aqueous buffer, which was lower than that of the wild-type peptide. Nevertheless, these data confirm that all gramicidin S analogues operate by the same fundamental antimicrobial mechanism, and hence, any structural or functional insights from the labelled peptides will also apply to the wild-type peptide.

Electrostatic interactions of PGLa with lipid bilayers

We will now describe several ^{19}F NMR experiments that are suitable for monitoring the lipid – protein interactions of the 4F-Phg-labelled peptides. As an example, we examine the role of negatively charged lipids on the binding and immersion of PGLa in model membranes. Like many other antimicrobial sequences, PGLa carries multiple positive charges along one side of an amphiphilic helix.[12, 13b] Electrostatic effects are assumed to play an important role in the selective recognition of negatively charged bacterial membranes; this mechanism provides a self-protective discrimination against eukaryotic cell surfaces.[1, 27] Nevertheless PGLa also binds to uncharged membranes, such as erythrocytes, through its hydrophobic side chains, albeit

 © 2003 Wiley-VCH Verlag GmbH & Co. KGaA, Weinheim

with a lower affinity. For example, the CD spectrum of the peptide in aqueous solution changes towards a more α-helical conformation in the presence of neutral DMPC vesicles (data not shown). The actual role of negatively charged lipids for the initial peptide binding and for further interactions with PGLa and related antimicrobial peptides is not yet completely understood.

^{19}F NMR spectroscopy of fluorine-labelled peptides can contribute in at least two ways to resolve this issue. First, solid-state NMR spectroscopy of peptides in macroscopically oriented membrane samples provides information about the alignment and dynamics of the peptide in the membrane-bound state.[5b, 6b–e] This information is encoded in the anisotropic chemical shift, linewidth and lineshape of the ^{19}F NMR signal when an oriented sample is measured at different tilt angles with respect to the magnetic field. To examine the electrostatic effect of the negatively charged lipid DMPG, we reconstituted the three L-4F-Phg-labelled PGLa analogues in zwitterionic DMPC bilayers with varying ratios of DMPG. The observed ^{19}F NMR anisotropic chemical shifts reflect the alignment of each labelled segment in the membrane. The values collected in Table 4 obviously differ for the three different labelled positions (Ala8, Ala10, Ile13). Remarkably, the respective chemical shifts remained very similar upon increasing the density of negative lipids in the membrane, a result suggesting that the peptide does not change its structure or alignment in response to the lipid head-group charge. We also compared samples with other peptide:lipid ratios and carried out controls with the epimers containing D-4F-Phg. Within any of these sets of data the chemical shift differences were hardly influenced by the ratio of DMPC:DMPG. The biggest deviation of about 4 ppm was observed for PGLa-10-L (Figure 7). Differences in the same range were observed due to variations in the peptide:lipid ratio in uncharged DMPC membranes.[29]

Table 4. Anisotropic ^{19}F NMR chemical shifts (in ppm) of PGLa analogues labelled with L-4F-Phg, reconstituted in orientated DMPC membranes with different ratios of negatively charged DMPG at a peptide:lipid molar ratio of 1:100. Membranes were aligned horizontally (H) or vertically (V) in the magnetic field.[a]

	PGLa-8-L		PGLa-10-L		PGLa-13-L	
	H	V	H	V	H	V
1:100 DMPC	−116.4	−110.4	−96.5	−121.4	−114.8	−114.9
1:80/20 DMPC/DMPG	−117.4	−109.9	−99.3	−120.3	−112.6	−115.8
1:60/40 DMPC/DMPG	n.d.[b]	n.d.[b]	−100.8	−119.8	−113.9	−115.3

[a] Each of the 9 samples was measured at 35 °C. The chemical shift of a sample can be measured with an accuracy of about 0.2 ppm, while differences between individual samples of identical composition can be up to 2 ppm.[29] [b] n.d. = not determined. The PGLa-8-L sample at 60/40 DMPC/DMPG showed broad NMR signals indicative of peptide aggregation.

At this point we shall not attempt to interpret the anisotropic chemical shift data in terms of the molecular structure and alignment in the membrane, as the necessary information about the rotameric state and side-chain dynamics of L-4F-Phg in PGLa is not yet fully available. Nevertheless, the results presented here allow a number of conclusions:

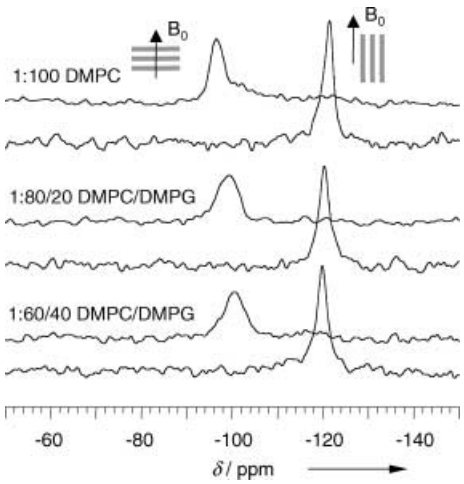

Figure 7. Solid-state ^{19}F NMR spectra of oriented membranes containing the antimicrobial peptide PGLa-10-L. Three samples with different ratios of DMPC:DMPG were measured with the membranes aligned either horizontally or vertically in the magnetic field. Each sample contains 0.33 mg of peptide and about 11 mg of phospholipid (peptide:lipid molar ratio = 1:100). Measurement time was 1 – 3 h per spectrum.

1) The ^{19}F NMR spectra consist of a single sharp peak, which indicates a uniform population of orientational states of PGLa. We cannot exclude, however, that PGLa might assume two or more different orientations—for example, on a flat membrane and in a pore—if those orientational states are in fast exchange with rate constants $\gg 10^3\ s^{-1}$, so that we observe only an average signal in the NMR experiment.

2) In the liquid-crystalline phase of the membrane PGLa must undergo fast rotation around the bilayer normal, because otherwise we would have observed a broad lineshape for the vertically tilted samples. This observation rules out the formation of large oligomers, at least for peptide:lipid ratios below 1:50. PGLa probably exists as a monomer or dimer under the conditions studied, just like many other membrane-associated peptides such as gramicidin S, B18, gramicidin A and protegrin-1.[6, 30]

3) The alignment of PGLa is not much influenced upon increasing the DMPG content from 0 to 40%, as otherwise we would have observed a pronounced shift in at least one of the three ^{19}F labels.

In the above experiments with oriented membrane samples it is clear that the partitioning of PGLa between the aqueous phase and the lipid bilayer does not play any significant role. As there is virtually no bulk phase of free water present in these (fully hydrated) samples, even a peptide with a very low affinity will be completely bound to the membrane. To gain more insight into the partitioning equilibrium and how it is influenced by electrostatics, we prepared a different set of samples containing unilamellar lipid vesicles that are suspended in excess aqueous solution. The binding of the ^{19}F-labelled PGLa peptides to such model membranes can thus be followed by solution-state ^{19}F NMR spectroscopy, which provides information about some thermodynamic and kinetic binding parameters. We monitored

 © 2003 Wiley-VCH Verlag GmbH & Co. KGaA, Weinheim

the ^{19}F NMR signal of PGLa-10-L as a function of increasing concentration of unilamellar DMPC/DMPG vesicles. When the negatively charged lipid vesicles are added stepwise to the sample tube, the integral of the ^{19}F NMR signal progressively decreases and finally disappears. This shows that by solution-state NMR spectroscopy we observe only the free form of the peptide. Any peptide bound to the vesicles gives rise to a signal that is several orders of magnitude broader (up to 20 ppm, corresponding to the chemical shift difference between the two sample orientations shown in Figure 7) and cannot be distinguished from the baseline.

To characterise the binding quantitatively, we titrated a concentrated PGLa-10-L stock solution into vesicle suspensions of different DMPC:DMPG ratios (Figure 8). Within the accuracy of our measurement we observed a fairly linear saturation behaviour, that is, all of the peptide was immediately captured by the charged vesicles up to a certain limiting amount. Any subsequently added peptide remained free in solution. If we wanted to determine the binding constant, we would have to analyse the exact curvature around the point of inflection, where the concentration of free peptide is in the order of the binding constant. However, this concentration range cannot be reliably addressed in this system because of the intrinsically low sensitivity of the NMR method. The MIC value of PGLa towards susceptible bacteria is 3 μM or below (Table 3), a fact suggesting an apparent binding constant of the same order of magnitude. The accuracy of integrating the ^{19}F NMR signal is about ± 10 μM for the signal-to-noise ratio achieved within a typical measurement time of 1 hour. Despite the relatively high sensitivity of the ^{19}F nucleus, this is not sufficient to determine the concentration of free peptide below and around the saturation point. It is therefore not possible to determine the apparent affinity constant for peptides with such high affinities by solution-state NMR spectroscopy.

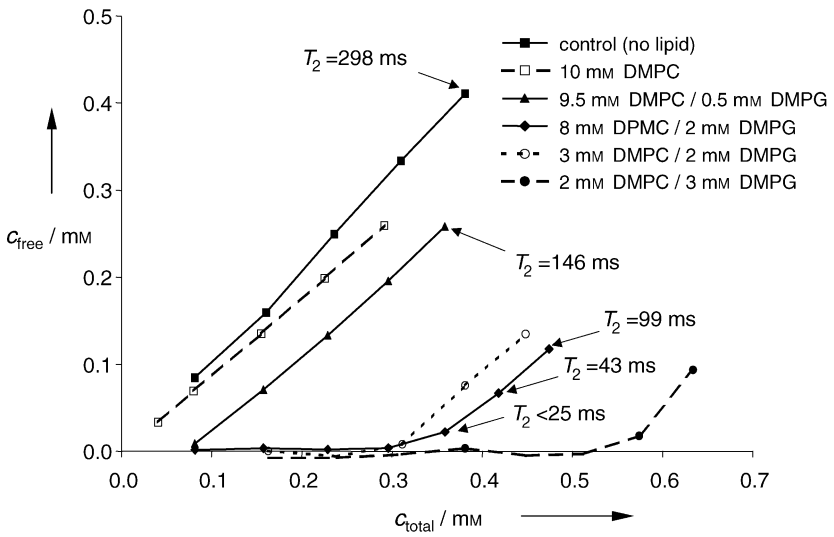

Figure 8. *Plot of the free-peptide concentration, c_{free} (determined from the ^{19}F NMR signal intensity in solution), as a function of the total amount of PGLa-10-L, c_{total}, titrated to suspensions of vesicles made from DMPC/DMPG mixtures containing different ratios of uncharged to negatively charged lipid. The measurement time was 20 – 50 minutes for each concentration data point and 1 – 2 h for each T_2 value.*

As seen in Figure 8, PGLa shows very little binding to uncharged vesicles composed of 100% DMPC. In the presence of DMPG the saturating amount of membrane-bound peptide correlates roughly with the total number of charged lipid head groups, if it is assumed that PGLa carries about five positive charges. In liquid-crystalline bilayers we can exclude the possibility that a cluster of DMPG molecules would form a distinct binding site for PGLa. The influence of the DMPG concentration on the binding of PGLa must rather be attributed to an overall electrostatic attraction that changes the local peptide concentration at the membrane surface. In a neutral DMPC bilayer the accumulation of positively charged amphiphilic peptides soon leads to electrostatic repulsion. The peptide concentration near the surface thus becomes lower than in the bulk solution, and equilibrium is reached despite a high concentration in the bulk. A negatively charged membrane, on the other hand, attracts the positively charged peptides to the surface and readily accommodates many more molecules before the charges are neutralised and equilibrium is attained.

Solution-state ^{19}F NMR spectroscopy can provide further kinetic information over three windows of time. First, our observation that the peptide signal loses its integral intensity upon adding the vesicles suggests that any exchange between the free and bound forms must be slower than about 10^4 s^{-1}. Otherwise, in the case of fast exchange between free and vesicle-bound peptide, the signal would have broadened without loss of integral intensity. Second, there are no binding processes with time constants of 10^{-2} – 10^{-5} s^{-1}, such as a slow trans-bilayer flip-flop. This is shown because we obtained the same results when measuring the concentration of free peptide immediately (a few minutes) after adding the vesicles and when repeating the measurement after hours or days. A third time window is accessible through the transverse relaxation time T_2. We measured the signal decay of a single echo NMR experiment as a function of the echo delay time. If any of the free peptide gets bound to the membrane during this delay, the corresponding ^{19}F magnetisation will lose its phase coherence. Even if the peptide is released again at the end of the delay, it can no longer contribute to the echo intensity. In these relaxation experiments we observed a dramatic reduction of T_2 from 300 ms in the absence of vesicles down to <25 ms in the presence of vesicles (Figure 8). Given the 100-ms range of the echo delay times, we conclude that the exchange between free and bound peptide occurs with a time constant in the order of 10 s^{-1}.

Conclusions

We have shown that the non-natural amino acid 4F-Phg can be readily incorporated into synthetic peptides by standard Fmoc solid-phase protocols, thereby providing a highly sensitive label for ^{19}F NMR studies of lipid – peptide interactions. Since racemisation of

 © 2003 Wiley-VCH Verlag GmbH & Co. KGaA, Weinheim

4F-Phg cannot be avoided, the peptides containing the L and D enantiomers have to be separated by reversed-phase HPLC in a TFA-free solvent. Using various functional assays on the different types of peptides, we have demonstrated that hydrophobic amino acids may generally be substituted by L-4F-Phg without any significant loss of biological activity. The epimeric peptides containing D-4F-Phg, on the other hand, showed differential responses that may yield information about the transient secondary structures required for function. For example, the sterically constrained side chain of D-4F-Phg interferes with the α-helical fold of PGLa, whereas it can be accommodated in every alternate position of the cyclic β sheet of gramicidin S. It will be interesting to see whether D-4F-Phg inhibits the self-assembly of oligomeric β sheets, as its stiff aromatic side chain might be a more efficient steric barrier for β-sheet formation than any natural amino acid that is flexible around $C\alpha-C\beta-C\gamma$. The racemised "byproduct" from peptide synthesis (containing the D-4F-Phg analogue) may thus find useful applications both in functional studies to probe transient conformations and as a component of rationally designed oligomerisation inhibitors against amyloid diseases.

The L-4F-Phg side chain serves as a highly sensitive and background-free reporter for ^{19}F NMR experiments on membrane-binding peptides. The stiff connection of the label to the peptide backbone makes it ideal for distance measurements, and the broad CSA tensor can be used as a probe for peptide orientation and dynamics both in solution- and solid-state NMR experiments. In macroscopically oriented membranes we typically acquire spectra from 0.33 mg of ^{19}F-labelled peptide in about 3 h; this compares very favourably with analogous solid-state NMR experiments on ^{2}H, ^{13}C or ^{15}N nuclei, which are 10–100-fold less sensitive.[6c] Even though the sensitivity of the solution-state ^{19}F NMR experiments was not yet high enough to determine directly a binding constant in the μM range, various time windows could be addressed to describe the reversible interactions of the peptide with lipid vesicles. In the case of the cationic antimicrobial peptide PGLa, we found that electrostatic interactions determine the initial membrane binding in solution, but once it is associated with the bilayer the presence of charged lipid head groups makes no difference to the alignment or mobility of the peptide. This finding may have important consequences for our understanding of the functional mechanism of PGLa and related peptides.

Experimental Section

Materials: Fmoc-L-ornithine(dde)-OH and Fmoc-D-phenylalanine were purchased from Bachem (Heidelberg, Germany; Fmoc = 9-fluorenylmethoxycarbonyl, dde = 1-(4,4-dimethyl-2,6-dioxocyclohex-1-ylidene)ethyl). Tetramethylfluoroformamidinium hexafluorophosphate (TFFH) was obtained from Advanced Chemtech (Louisville, KY), and 2-(1*H*-benzotriazole-1-yl)-1,1,3,3-tetramethyluronium hexafluorophosphate (HBTU) was from Richelieu Biotechnologies (Montreal, Canada). Diethyl ether, acetone, acetonitrile, methanol and *N*,*N*-dimethylformamide (DMF; synthesis grade) were obtained from Roth (Karlsruhe, Germany). DMF was purified by standard methods.[31] *N*-2-hydroxyethylpiperazine-*N*′-2-ethanesulfonic acid (HEPES) was obtained from Sigma, and *N*,*N*-diisopropylethylamine (DIEA), trifluoroacetic acid (TFA), triisopropylsilane (TIS), trifluoroethanol (TFE), *N*-methylpyrrolidine (NMP), α-cyano-4-hydroxycinnamic acid, piperidine, sodium fluoride and fluorotrichloromethane were obtained from Aldrich. The compounds 2,4,6-collidine, 4-fluoro-L-α-phenylglycine (L-4F-Phg), 4-fluoro-DL-α-phenylglycine (D/L-4F-Phg) and hydrazine were obtained from Fluka (Taufkirchen, Germany), while tetrahydrofuran (THF) was from Merck (Darmstadt, Germany). All other chemicals for peptide synthesis were purchased from Calbiochem-Novabiochem (Bad Soden, Germany). 1-Fluoro-2,4-dinitrophenyl-5-L-alanine amide (Marfey's reagent) was obtained form Pierce (Bonn, Germany). N-terminal Fmoc protection of L-4F-Phg and D/L-4F-Phg was performed with Fmoc-Cl as previously reported.[32]

The lipids 1,2-dimyristoyl-*sn*-glycero-3-phosphocholine (DMPC) and 1,2-dimyristoyl-*sn*-glycero-3-[phospho-*rac*-(1-glycerol)] (DMPG), as well as the fluorescence-labelled lipids L-α-phosphatidylethanolamine-*N*-(lissamine rhodamine B sulfonyl) and L-α-phosphatidylethanolamine-*N*-(4-nitrobenzo-2-oxa-1,3-diazole), were obtained from Avanti Polar Lipids (Alabaster, AL). All chemicals used were of the highest grade and were used as received unless otherwise mentioned.

Peptide synthesis: Peptides were synthesised either on an Applied Biosystems 433A instrument, on an Abimed Economy Peptide Synthesizer EPS 221, or manually by using standard solid-phase Fmoc protocols.[33] Deprotection was carried out with 20% piperidine in DMF, and preactivation was performed with 1-hydroxy-1*H*-benzotriazole (HOBt) and HBTU in the presence of the base DIEA. NMP or DMF were used as solvents. The deprotection and coupling efficiency was monitored by performing a Kaiser test.[34] The protected peptides were cleaved from the resin at room temperature by treatment with a cocktail of TFA (95%), water (2.5%) and TIS (2.5%) for 2–5 h with occasional shaking. In the case of gramicidin S we had to use 5% TIS to avoid alkylation by cations produced during cleavage. The resin was filtered off and washed with pure TFA. The combined filtrates were evaporated to a reduced volume under a gentle stream of nitrogen. The crude product was precipitated with cold diethyl ether, taken up in acetonitrile/water (1:9) and lyophilised.

In our attempts to suppress racemisation of L-4F-Phg, the synthesis was performed in an automated manner only up to the stage of introducing the label. The fluorinated amino acid and the following one were then introduced manually as described in the Results and Discussion section. The remaining sequence was then completed on the peptide synthesizer.

In the cyclisation of gramicidin S, the linear peptide (0.5 mg mL^{-1}) was dissolved in dry degassed dichloromethane (DCM) in a 50-mL round-bottomed flask. Solid pyridinium 1-benzotriazolyloxytris(dimethylamino)phophonium hexafluorophosphate (3 equiv to the peptide) and a solution of HOBt (3 equiv) in degassed DMF (0.5 mL) were added to the flask, and the mixture was stirred. DIEA (6 equiv) was then added to initiate the reaction. The reaction was monitored by HPLC and allowed to proceed overnight under an argon atmosphere. After removing the DCM by rotary evaporation, ethyl acetate (30 mL) was added and the remains of the DMF were washed off with water (2 × 30 mL). The organic layer was dried over Na_2SO_4 and the solvent was removed by rotary evaporation to obtain an oil. This oil was taken up in ethyl acetate, lyophilised and purified by HPLC.

The cyclised product still had the dde protecting group on the ornithine residues. For the deprotection the peptide was taken up in THF and treated with hydrazine solution (2% v/v in THF). The mixture was stirred for about 2 h at room temperature before being left at

 © 2003 Wiley-VCH Verlag GmbH & Co. KGaA, Weinheim

−73 °C overnight to precipitate the removed dde as the oxazolone. The precipitate was filtered and the solvent was removed from the filtrate by rotary evaporation to give another yellowish oil, which was dissolved in acetonitrile/water (1:1, 3 mL) and lyophilised. Mass spectrometry on this sample provided evidence of proper cyclisation and complete removal of the dde protecting group. The crude product was further purified by HPLC before use.

HPLC purification of peptides: Peptides were purified with reversed-phase HPLC (Jasco, Japan; 10 × 250 mm Vydac C18 columns; flow rate of 6 mL min^{-1}). Water/acetonitrile gradients were individually optimised at 30–40 °C for each peptide analogue. B18 and gramicidin S analogues were purified in a single step, with the amount of deletion peptides and of other side products being between 5 and 15%. PGLa analogues were purified in two steps: the epimers were first separated with 0.1% TFA in both phases and, following lyophilisation, they were further purified in TFA-free solvent, thereby reducing the amount of deletion peptides to less than 3%. For all peptides the last HPLC step was performed with 5 mM HCl in the aqueous phase and pure acetonitrile as the organic phase. All samples prepared for this ^{19}F NMR study contained less than 0.1 mole of TFA per mole of peptide as judged by the ^{19}F NMR peak intensities in solution.

Mass spectrometry: The identity of the peptides was confirmed with mass spectrometry. We used electrospray ionisation (ESI) and/or matrix-assisted laser desorption/ionisation time-of-flight (MALDI-TOF) spectrometry. Samples for ESI were dissolved in 99% methanol and measured on a Fisons VG Quattro triple quadrupole mass spectrometer. MALDI-TOF samples were cocrystallised with a matrix of α-cyano-4-hydroxy-cinnamic acid from acetonitrile/water solutions onto a stainless steel target. Measurements were made on a Bruker Reflex 2 instrument. When both techniques were successfully employed, we found identical results.

Assignment of L- and D-4F-Phg enantiomers: Samples of purified peptide (0.2 mg) were hydrolysed with 6 M HCl (0.5 mL) for 16 h at 105 °C. The amino acids were derivatised with Marfey's reagent:[22] the HCl was removed by lyophilisation, 0.5 M $NaHCO_3$ (25 μL) and 1% Marfey's reagent in acetone (50 μL) were added, the mixture was incubated at 40 °C for 90 min, and finally 2 M HCl (7 μL) was added. The mixture of the derivatised amino acids was resolved by analytical HPLC (4.6 × 250 mm Vydac C18 column; flow rate of 1.5 mL min^{-1}; detection at 415 nm) at 40 °C with a linear acetonitrile/water gradient containing 0.1% TFA, from 10 to 43% acetonitrile over 12 min. Peaks were identified by comparison with chromatograms of pure derivatised L- and D-4F-Phg (see Figure 2).

High-resolution ^{1}H NMR spectroscopy: Samples of 1.8–2.4 mM PGLa were prepared in an aqueous solution (350 μL) containing 30% TFE-d_3, 10 mM potassium phosphate buffer (pH 7.0 before TFE addition), 0.05% NaN_3 and 0.1 mM 3-(trimethylsilyl)propionic acid-d_4 and measured into 5-mm tubes between Doty susceptibility plugs. Two-dimensional ^{1}H–^{1}H TOCSY (100 ms mixing time; 8 h measurement time) and NOESY spectra (150 ms; 16–32 h) were recorded with WATERGATE water suppression on a 600 MHz Unity Inova spectrometer (Varian, Palo Alto, CA) with standard equipment. The spectra were evaluated with the programs NMRPipe, SPSCAN and XEASY,[35] and molecular models were created and visualised with SYBYL (Tripos, St. Louis, MO) and MOLMOL.[36] Ring-current shifts were determined according to the Johnson–Bovey model, as implemented in MOLMOL.

Fluorescence assay for fusogenic activity: The peptide-induced fusion of large unilamellar vesicles (LUVs) was monitored with a fluorescence dequenching assay, as previously reported.[15b] LUVs of brain sphingomyelin/cholesterol (80:20 molar ratio) with and without 0.8 mol% of both the fluorescence-labelled lipids L-α-phosphatidylethanolamine-*N*-(lissamine rhodamine B sulfonyl) and L-α-phosphatidylethanolamine-*N*-(4-nitrobenzo-2-oxa-1,3-diazole) were produced in a lipid extruder (Avestin, Canada) with Poretics polycarbonate membranes of 100-nm pore diameter (Osmonics, Livermore, CA). 40 μM $ZnCl_2$ and 2 μM B18 peptide were added to trigger fusion, and the fluorescence intensity was monitored with an LS 50B luminescence spectrometer (Perkin Elmer) with the excitation set at 465 nm and the emission set at 520 nm. The initial rate of fusion was determined from an exponential fit to the increase in fluorescence intensity 3–30 seconds after addition of peptide, and was compared with the total increase after addition of Triton X100.

Antimicrobial inhibition assays: As test organisms for antimicrobial activity assays we used the Gram-negative bacteria *Escherichia coli* ATCC 25922, *E. coli* DC2 (antibiotic-susceptible penetration mutant),[37] *Pseudomonas aeruginosa* ATCC 9027, *P. aeruginosa* K799/61 (antibiotic-susceptible penetration mutant),[38] *Burkholderia cepacia* DSM 7288 (resistant to cationic peptides),[39] *B. vietnamiensis* DSM 11319, *B. multivorans* BF7 (clinical isolate obtained from Prof. Dr. A. Bauernfeind, MICOER-Institute, Munich, Germany) and the Gram-positive bacteria *Staphylococcus aureus* SG511, *S. aureus* 134/93 (MRSA),[40] *Bacillus subtilis* ATCC 6633, *Micrococcus luteus* ATCC 10240 and ATCC 9341, *Mycobacterium vaccae* IMET 10670, and *Mycobacterium fortuitum* B.

Antibacterial activity was determined qualitatively by agar diffusion tests[24] and quantitatively by measurement of MIC values in liquid-growth inhibition assays.[25] For agar diffusion assays, a suspension (100 μL) of the test organism with a density of McFarland standard 1 was inoculated into sterile melted 1% Trypticase soy broth (TSB) agarose (32 mL), cooled to 50 °C and then poured into Petri dishes. The final concentration of cells was 10^6 colony-forming units (CFU) per mL. Each antimicrobial peptide (50 μL) at a concentration of 100 μg mL^{-1} was filled into 9-mm holes that had been cut out of the agar (5 μg of peptide per hole). The diameter of the zone of inhibition around the hole in mm was determined after 24 h of incubation at 37 °C.

Minimum inhibitory concentration (MIC) values were determined by using a standard microbroth dilution method in 1% TSB.[25] The cells were grown overnight at 37 °C in nutrient broth and then diluted in TSB. The peptide solutions (50 μL) were serially diluted by a factor of two with TSB, and then the wells were inoculated with bacteria (50 μL) to give a final concentration of 5×10^5 CFU mL^{-1} in a volume of 100 μL, unless stated otherwise. Microtiter plates were incubated at 37 °C for 24 h and read with a Nepheloscan Ascent 1.4 automatic plate reader (Labsystems, Vantaa, Finland). All experiments were performed in triplicate. MIC values are stated as the lowest antibiotic concentration that inhibited growth.

Solid-state ^{19}F NMR spectroscopy: NMR measurements were performed on a 500 MHz wide-bore Unity Inova spectrometer (Varian, Palo Alto, CA). For solid-state ^{19}F NMR spectroscopy, a ^{19}F/^{1}H double-tuned flat-coil probe head with a goniometer (Doty Scientific Inc., Columbia, SC) and an external 470 MHz high-power amplifier (Creative Electronics Inc., Los Angeles, CA) were used.[4a, 7b]

Oriented membrane samples were prepared by depositing peptide–lipid mixtures on cleaned and vacuum-dried glass slides (0.08 × 7.5 × 18 mm^3, Marienfeld Inc., Germany).[6b–d] The peptide was dissolved in water and the lipid in methanol. Both components were then mixed to give a 70% methanol solution containing about 20–100 mg mL^{-1} of material in total. Drops (20–30 μL) were spread onto each glass plate (the number of plates necessary depends on the desired peptide:lipid ratio, typically 8 plates were used for 0.33 mg of PGLa in a 1:100 peptide:lipid ratio). After initial drying in a laminar flow

 © 2003 Wiley-VCH Verlag GmbH & Co. KGaA, Weinheim

bench, the membrane films were dried to completion under vacuum overnight. The plates were stacked and hydrated for 2 days at 48 °C in an atmosphere over a saturated K_2SO_4 solution (about 96% relative humidity). The stack was wrapped in parafilm and polyethylene film to maintain the hydration of the sample during the NMR measurement. ^{1}H-decoupled ^{31}P NMR spectra were recorded to judge the quality of bilayer orientation in the samples. The well-oriented lipid typically contributed 80–95% to the total ^{31}P NMR phospholipid signal.

Peptide–lipid interactions studied by ^{19}F NMR in solution: LUVs were prepared from DMPC or DMPC/DMPG mixtures in 10 mM HEPES buffer (pH 7.0) with 1 mM NaF, as described for the fusion assays above. Small unilamellar vesicles were prepared by ultrasonication of the lipid suspension. The vesicles were mixed with peptide stock solution, and the mixture (0.6 mL) was filled into 5-mm NMR tubes for high-resolution measurements. ^{19}F NMR free induction decays were recorded immediately after a 90° pulse at 470 MHz, with a standard triple-resonance probe head for high-resolution measurements (Varian, Palo Alto, CA), where the proton channel was tuned to fluorine. Fluorine chemical shifts were referenced to external $CFCl_3$ with a thin capillary filled with pure $CFCl_3$ extending over the full length of the tube. After Fourier transformation, the NMR signal intensity of the labelled peptide was determined by integration over a range ± 0.12 ppm from the peak maximum after visual phasing and linear baseline correction for the outermost 10% of a ± 1 ppm range. This was compared with the integral of the NaF signal.

Acknowledgements

We thank Sigrid Reichardt, Waltraud Scheiding and Irmgard Heinemann for excellent technical support, and we gratefully acknowledge Charles Glabe (University of California, Irvine) for having provided the Arg- and His-substituted B18 analogues. This work was supported by the Deutsche Forschungsgemeinschaft within program SFB 197 (TP B13).

Keywords: amphiphilic peptides · biomembranes · fluorine · fluorophenylglycine · NMR spectroscopy

[1] a) R. E. W. Hancock, D. S. Chapple, *Antimicrob. Agents Chemother.* **1999**, *43*, 1317–1323; b) M. Zasloff, *Nature* **2002**, *415*, 389–395; c) Y. Shai, *Curr. Pharm. Des.* **2002**, *8*, 715–725.

[2] E. I. Pécheur, J. Sainte-Marie, A. Bienvenüe, D. Hoekstra, *J. Membrane. Biol.* **1999**, *167*, 1–17.

[3] R. R. Ketchem, K. C. Lee, S. Huo, T. A. Cross, *J. Biomol. NMR* **1996**, *8*, 1–14.

[4] a) S. L. Grage, A. S. Ulrich, *J. Magn. Reson.* **1999**, *138*, 98–106; b) A. S. Ulrich in *Encyclopedia of Spectroscopy and Spectrometry* (Eds.: J. Lindon, G. Trautner, J. Holmes), Academic Press, **2000**, 813–825; c) M. L. Gilchrist, Jr., K. Monde, Y. Tomita, T. Iwashita, K. Nakanishi, A. E. McDermott, *J. Magn. Reson.* **2001**, *152*, 1–6.

[5] a) J. T. Gerig, *Prog. in NMR*. **1994**, *26*, 293–370; b) S. L. Grage, J. Salgado, U. Dürr, S. Afonin, R. W. Glaser, A. S. Ulrich in *Perspectives on Solid State NMR in Biology* (Eds.: S. Kiihne, H. J. M. de Groot), Kluwers Academic Press, Dordrecht, **2001**, 83–91.

[6] a) M. A. Danielson, J. J. Falke, *Annu. Rev. Bioph. Biomol. Struct.* **1996**, *25*, 163–195; b) J. Salgado, S. L. Grage, L. H. Kondejewski, R. S. Hodges, R. N. McElhaney, A. S. Ulrich, *J. Biomol. NMR* **2001**, *21*, 191–208; c) S. L. Grage, J. Wang, T. A. Cross, A. S. Ulrich, *Biophys. J.* **2002**, *83*, 3336–3350; d) S. Afonin, U. Dürr, R. W. Glaser, A. S. Ulrich, *Magn. Res. Chem.* **2004**, in press; e) O. Toke, R. D. O'Connor, W. L. Maloy, R. W. Glaser, A. S. Ulrich, J. Schaefer, unpublished results.

[7] a) P. Tang, B. Yan, Y. Xu, *Biophys. J.* **1997**, *72*, 1676–1682; b) S. L. Grage, A. S. Ulrich, *J. Magn. Reson.* **2000**, *146*, 81–88.

[8] U. N. Sundram, J. H. Griffin, *J. Am. Chem. Soc.* **1996**, *118*, 13 107–13 108; b) J. M. Janusz, J. M. Gardlik, P. A. Young, R. V. Burkes, S. J. Stoll, A. F. Estelle, C. M. Riley, *J. Med. Chem.* **1990**, *33*, 1052–1061; c) W. M. Kati, D. Montgomery, C. Maring, V. S. Stoll, V. Giranda, X. Chen, W. G. Laver, W. Kohlbrenner, D. W. Norbeck, *Antimicrob. Agents Chemother.* **2001**, *45*, 2563–2570; d) S. Abu-Lafi, S. A. Turujman, *J. Chromatogr. A.* **1999**, *855*, 157–170.

[9] a) M. J. Anteunis, R. E. Callens, D. K. Tavernier, *Eur. J. Biochem.* **1975**, *58*, 259–268; b) Y. Lee, R. B. Silverman, *Fourth International Electronic Conference on Synthetic Organic Chemistry* (ECSOC-4), **2000**, www.mdpi.org/ecsoc-4.htm.

[10] K. Ramanarayan, M. F. Chan, V. N. Balaji, S. Profeta, S. N. Rao, *Int. J. Peptide Protein Res.* **1995**, *45*, 366–376.

[11] a) E. Krause, M. Bienert, P. Schmieder, H. Wenschuh, *J. Am. Chem. Soc.* **2000**, *122*, 4865–4870; b) Y. Chen, C. T. Mant, R. S. Hodges, *J. Pept. Res.* **2002**, *59*, 18–33.

[12] B. Bechinger, M. Zasloff, S. J. Opella, *Biophys. J.* **1998**, *74*, 981–987.

[13] a) M. E. Houston, L. H. Kondejewski, D. N. Karunaratne, M. Gough, S. Fidai, R. S. Hodges, R. E. Hancock, *J. Peptide Res.* **1998**, *52*, 81–88; b) K. Matsuzaki, *Biochim. Biophys. Acta* **1999**, *1462*, 1–10; c) J. A. Whiles, R. Brasseur, K. J. Glover, G. Melacini, E. A. Komives, R. R. Vold, *Biophys. J.* **2001**, *80*, 280–293; d) M. Dathe, H. Nikolenko, J. Meyer, M. Beyermann, M. Bienert, *FEBS Lett.* **2001**, *501*, 146–150.

[14] a) S. E. Hull, R. Karlsson, P. Main, M. M. Woolfson, E. J. Dodoson, *Nature* **1978**, *275*, 206–207; b) M. Jelokjani-Nirakai, E. J. Prenner, L. H. Kondejewski, C. M. Kay, R. N. McElhaney, R. S. Hodges, *J. Pept. Res.* **2001**, *58*, 293–306; c) M. Jelokjani-Nirakai, E. J. Prenner, C. M. Kay, R. N. McElhaney, R. S. Hodges, *J. Pept. Res.* **2002**, *60*, 23–36.

[15] a) P. L. DeAngelis, C. G. Glabe, *Peptide Res.* **1990**, *3*, 62–68; b) A. S. Ulrich, M. Otter, C. G. Glabe, D. Hoekstra, *J. Biol. Chem.* **1998**, *273*, 16 748–16 755.

[16] J. Yang, C. M. Gabrys, D. P. Weliky, *Biochemistry* **2001**, *40*, 8126–8137.

[17] a) R. W. Glaser, M. Grüne, C. Wandelt, A. S. Ulrich, *Biochemistry* **1999**, *38*, 2560–2569; b) A. S. Ulrich, W. Tichelaar, G. Förster, O. Zschörnig, S. Weinkauf, H. W. Meyer, *Biophys. J.* **1999**, *77*, 829–841.

[18] L. A. Carpino, A. El-Faham, *J. Am. Chem. Soc.* **1995**, *117*, 5401–5402.

[19] A. El-Faham, *Chem. Lett.* **1998**, *7*, 671–672.

[20] a) G. Karygiannis, C. Athanassopoulos, P. Mamos, N. Karamanos, D. Papaioannou, G. W. Francis, *Acta Chem. Scand.* **1998**, *52*, 1144–1150; b) L. A. Carpino, D. Sadat-Aalaee, H. G. Chao, R. H. DeSelms, *J. Am. Chem. Soc.* **1990**, *112*, 9651–9652.

[21] E. Krause, M. Beyermann, M. Dathe, S. Rothemund, M. Bienert, *Anal. Chem.* **1995**, *67*, 252–258.

[22] P. Marfey, *Carlsberg Res. Commun.* **1984**, *49*, 591–596.

[23] H. Binder, K. Arnold, A. S. Ulrich, O. Zschörnig, *Biochim. Biophys. Acta* **2000**, *1468*, 345–358.

[24] *Deutsches Arzneibuch*, 9th ed., Deutscher Apotheker Verlag, Stuttgart, **1990**, pp. 47–48 and 424–430.

[25] *Methods for dilution antimicrobial susceptibility tests for bacteria that grow aerobically*, 4th ed. (Villanova, PA, USA), National Committee for Clinical Laboratory Standards, **1997**, approved standard document M7 A4.

[26] a) D. Avrahami, Z. Oren, Y. Shai, *Biochemistry* **2001**, *40*, 12 591–12 603; b) S. Y. Hong, J. E. Oh, K. H. Lee, *Biochem. Pharmacol.* **1999**, *58*, 1775–1780.

[27] T. Wieprecht, M. Dathe, M. Schümann, E. Krause, M. Beyermann, M. Bienert, *Biochemistry* **1996**, *35*, 10 844–10 853.

[28] D. Wade, A. Boman, B. Wåhlin, C. M. Drain, D. Andreu, H. G. Boman, R. B. Merrifield, *Proc. Natl. Acad. Sci. USA* **1990**, *87*, 4761–4765; R. Besalle, A. Kapitkovsky, A. Gorea, I. Shalit, M. Fridkin, *FEBS Lett.* **1990**, *274*, 151–155.

[29] R. W. Glaser, A. S. Ulrich, *J. Magn. Reson.* **2003**, *164*, 104–114.

[30] S. Yamaguchi, T. Hong, A. Waring, R. I. Lehrer, M. Hong, *Biochemistry* **2002**, *41*, 9852–9862.

[31] D. D. Perrin, W. L. F. Amarego, *Purification of Laboratory Chemicals*, 3rd ed., Pergamon Press, Oxford, **1988**.

[32] L. A. Carpino, G. Y. Han, *J. Org. Chem.* **1972**, *37*, 3404–3409.

[33] a) C. D. Chang, J. Meienhofer, *Int. J. Peptide Protein Res.* **1978**, *11*, 246–249; b) G. B. Fields, R. L. Noble, *Int. J. Peptide Protein Res.* **1990**, *35*, 161–214.

[34] E. Kaiser, R. L. Colescott, C. D. Bossinge, P. I. Cook, *Anal. Biochem.* **1970**, *34*, 595–598.

 © 2003 Wiley-VCH Verlag GmbH & Co. KGaA, Weinheim

[35] a) F. Delaglio, S. Grzesiek, G. W. Vuister, G. Zhu, J. Pfeifer, A. Bax, *J. Biomol. NMR* **1995**, *6*, 277 – 293; b) T. Szyperski, B. Banecki, D. Braun, R. W. Glaser, *J. Biomol. NMR* **1998**, *11*, 387 – 405; c) C. Bartels, T. H. Xia, M. Billeter, P. Günthert, K. Wüthrich, *J. Biomol. NMR* **1995**, *2*, 619 – 629.
[36] R. Koradi, M. Billeter, K. Wüthrich, *J. Mol. Graphics* **1996**, *14*, 51 – 55.
[37] M. G. Richmond, D. C. Clarke, S. Wotton, *Antimicrob. Agents Chemother.* **1976**, *10*, 215 – 218.
[38] W. Zimmermann, *J. Clin. Pharmacol. Biopharm.* **1979**, *17*, 131 – 134.
[39] R. E. W. Hancock, *Lancet* **1997**, *349*, 418 – 422.
[40] W. Witte, C. Cuny, C. Braulke, D. Heuck. *Epidemiol. Infect.* **1994**, *113*, 67 – 73.
[41] G. Merutka, H. J. Dyson, P. Wright, *J. Biomol. NMR* **1995**, *5*, 14 – 24.

Received: January 31, 2003
Revised version: July 17, 2003 [F 568]

 © 2003 Wiley-VCH Verlag GmbH & Co. KGaA, Weinheim